

Tightening Dynamics of Wound Rolls: The Interplay of Solid Friction and Interfacial Compressibility Supplementary Material

M. Caelen, S. Moulinet, B. Andreotti, and F. Lechenault
*Laboratoire de Physique de l'Ecole Normale Supérieure, PSL, Sorbonne Université,
Université Paris Cité, CNRS, 24 rue Lhomond 75005 Paris, France.*

(Dated: February 11, 2025)

In this supplementary document, we present two theoretical derivations, describe certain experimental methodologies, and provide data pertaining to an alternative material for the roll (curling ribbon).

CAPSTAN EQUATION

We examine the capstan problem for a tape in the shape of an Archimedean spiral that slides uniformly along its entire length. We assume that the sliding friction adheres to Amontons-Coulomb's law, and we parameterize the tension as $\vec{T}(\theta) = T(\theta)\vec{e}_\theta$, where θ is the unwrap angle and \vec{e}_θ is the tangential unit vector. The force balance is given by:

$$\frac{d(T(\theta)\vec{e}_\theta)}{d\theta} = w (\vec{e}_{\theta+\pi/2} - \mu\vec{e}_\theta) (r(\theta)P(\theta) - r(\theta - 2\pi)P(\theta - 2\pi)) \quad (1)$$

with μ the dynamic friction coefficient. This equation simplifies to the Capstan equation:

$$\frac{dT}{d\theta} + \mu T = 0 \quad (2)$$

SENSITIVITY TO STRETCHING

Figure 2 of the article presents measurements of db/dx , where b is the outer radius of the roll and x is the length of the tape that has been pulled. These measurements indicate that the Super 8 tape can be considered inextensible under the applied tensions. To test the sensitivity to the tape's stretching, we hypothesise that the entire tape has a small relative elongation ϵ . The conservation of the tape's surface area is given by:

$$\pi(b^2 - a^2) = ((1 + \epsilon)L - x)h \quad (3)$$

where $h = (b - a)/N$ is the thickness, regardless of its origin, and L is the initial length of the roll. Consequently:

$$\pi N(b + a) = (1 + \epsilon)L - x \quad (4)$$

which leads to:

$$\pi N \frac{db}{dx} = \frac{d\epsilon}{dx} L - 1 \quad (5)$$

This equation provides a corrective factor $\frac{d\epsilon}{dx}L$ to the incompressible equation. In Figure (2) of the article, the statistical error bars correspond to a band of $\frac{d\epsilon}{dx} = \pm 0.2\%$ /m, demonstrating that the incompressibility test is highly sensitive.

MEASUREMENT OF THE SURFACE COMPRESSIBILITY

The surface compressibility is determined by compressing N stacked ribbon layers using an *Instron* force apparatus, equipped with custom-rectified plates to ensure precise parallelism. Both the compression load F_N and the displacement x_N of the compressing arm are measured. The measurement for a single layer ($N = 1$) serves as a reference to isolate and subtract the displacement attributable to the apparatus itself at the same applied force. Consequently, the measured interlayer spacing is defined as:

$$h = -\frac{x_{N+1}(F_{N+1}) - x_1(F_{N+1})}{N}. \quad (6)$$

This interlayer spacing is associated with the pressure $P = F_{N+1}/A$, where $A = w \times \ell$ represents the area of the ribbon segments. For the Super 8 tape (as discussed in the main article), the area is $A = w \times \ell = 8.0 \text{ mm} \times 100 \text{ mm}$. For the curling ribbons, which also exhibit a quasi-exponential growth of pressure with respect to interlayer spacing, the corresponding measurements are displayed in Fig. 1 with $w = 7 \text{ mm}$, resulting in an area of $A = 7.0 \text{ mm} \times 100 \text{ mm}$.

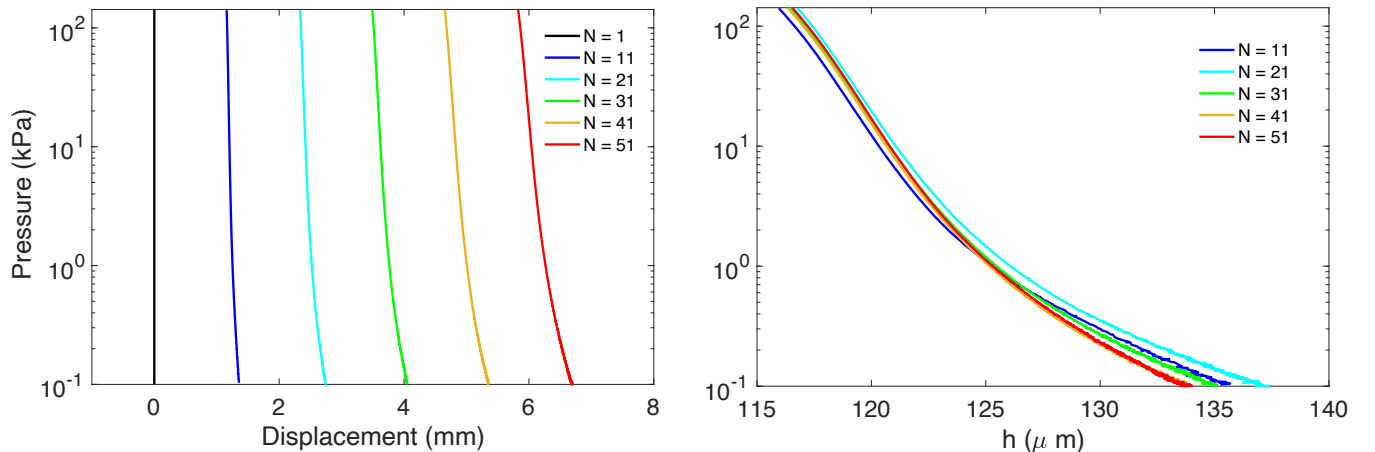


Figure 1. Left: Raw compression pressure as a function of absolute displacement for stacks of tapes with various numbers of layers, for 7 mm wide curling ribbon. Right: Same measurements where the x axis has been rescaled by the number of layers N following Eq. (6).

MEASUREMENT OF FRICTION COEFFICIENT

We constructed an inclined plate covered with tapes aligned parallel to the slope (length $\sim 75 \text{ cm}$, width $\sim 5 \text{ cm}$). A sliding mobile, consisting of a flat plate ($8 \text{ cm} \times 8 \text{ cm}$) with an attached smartphone, was prepared. The bottom of the mobile was covered with the same tapes, oriented parallel to those on the inclined plate.

To determine the static coefficient of friction, we placed the mobile in contact with the inclined plate and immediately released it. Depending on the angle of the plate, the mobile either remained stationary or slid down the slope. By identifying the critical inclination angle α that separates these two behaviors, we determined the static friction coefficient as $\mu_s = \tan \alpha$.

The dynamic coefficient of friction, μ_d , was obtained by placing the mobile on the plate at a fixed inclination angle β and allowing it to slide. We utilized the smartphone's accelerometers to measure the motion. Since the accelerometers do not distinguish between the acceleration \mathbf{a} of the smartphone and gravity \mathbf{g} , they record the quantity $\mathbf{m} = \mathbf{a} - \mathbf{g}$. If the mobile slides at a constant acceleration, the component of \mathbf{m} tangential to the plate is $m_{\parallel} = -\mu_d g \cos \beta$, and the normal component is $m_{\perp} = -g \cos \beta$. During the mobile's descent, the recording of m_{\parallel} exhibits a plateau, where the ratio m_{\parallel}/m_{\perp} yields the value of μ_d . Similar results were obtained by measuring the deceleration of the mobile after it was pushed on the horizontally positioned plate.

Table I compiles the measurements for two types of tape (Super 8 and curling ribbon). The uncertainties in μ_s reflect the reproducibility of the experiment, while those in μ_d arise from noise in the m_{\parallel} signal. For the curling ribbon, the difference between μ_s and μ_d was not assessed through these two independent measurements.

Table I. Measured values of the friction coefficients

coefficient	Super 8	curling ribbon
μ_s	0.31 ± 0.02	0.21 ± 0.02
μ_d	0.26 ± 0.03	0.21 ± 0.03

DATA FOR CURLING RIBBON

We replicated the tightening protocol for curling ribbons with two different widths (7 mm and 30 mm). Equation (3) of the letter remains valid for this distinct material, as illustrated in Fig. 2. Notably, the two ribbons of differing widths exhibit slightly varied average thicknesses, as evidenced by the compressibility measurements. The curling ribbons demonstrate a similar compressive response and dynamic behavior to the Super 8 video tape discussed in the main article. However, the thickness of the industrial curling ribbons is less well-controlled and is 1.6 times smaller than that of the Super 8 tape. Additionally, the material exhibits a Young's modulus of 1.6 GPa, which is 1.7 times lower than that of the Super 8 video tape. Overall, the curling ribbon is 7 times softer, yet retains the same phenomenological characteristics. The quantitative agreement is less pronounced than for the Super 8 video tape, which can be attributed to stretching effects and, more significantly, to material heterogeneity.

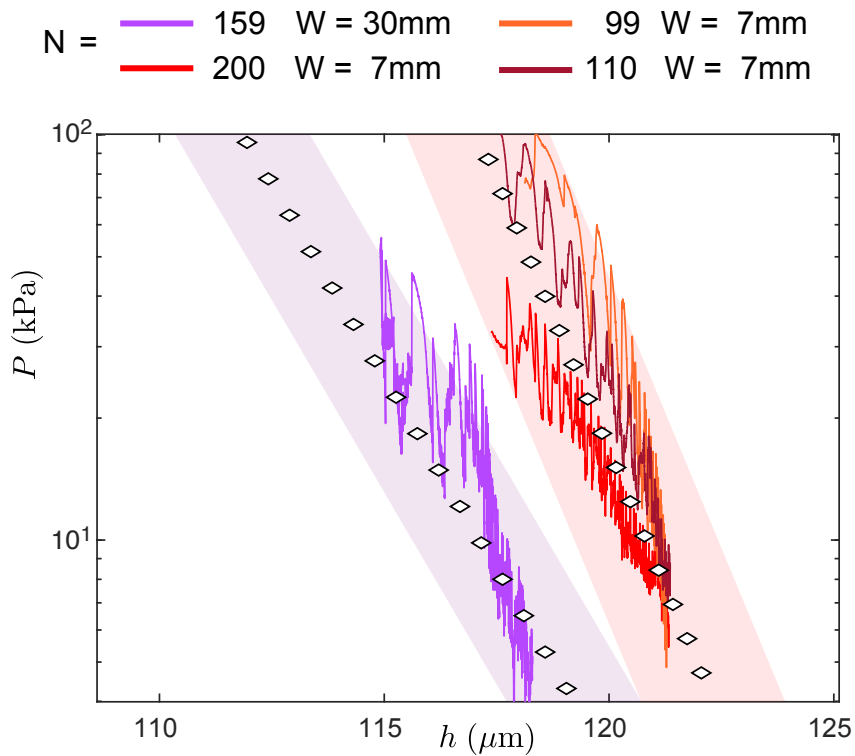


Figure 2. Combined tightening and compressibility measurements for two different widths of curling ribbon are presented. The diamonds represent the compression tests reported earlier. The coloured curves illustrate the tightening forces converted into pressures using Equation (3) from the main paper, with the thickness h determined from video measurements. The coloured bands represent the 1% systematic uncertainty on h in our image analysis.

AFM TOPOGRAPHY OF THE RIBBON

In order to characterize the roughness of the ribbon used in the core of the manuscript, we performed an AFM scan of a representative patch on the ribbon surface after it underwent a tightening experiment (Fig. 3). Scratches along the pulling direction (X-axis) can be observed.

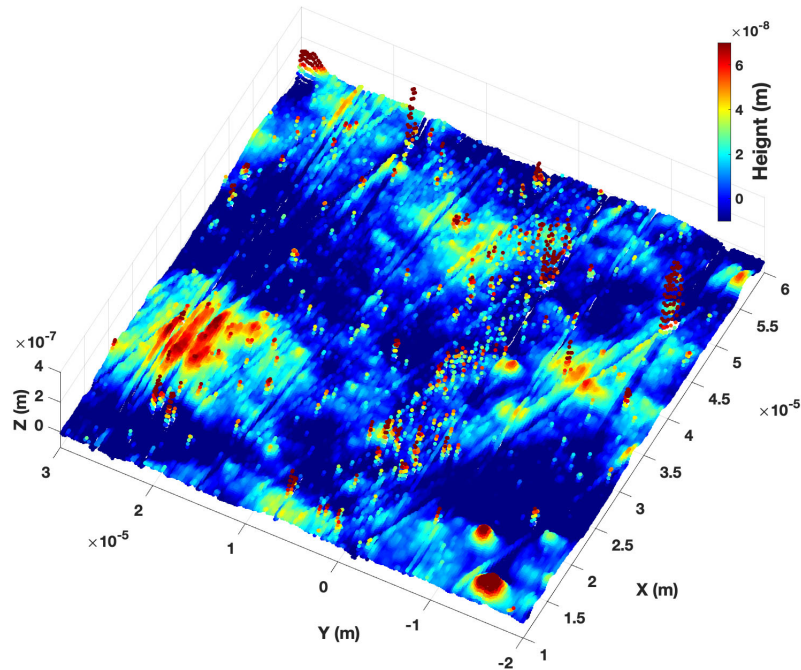


Figure 3. Typical AFM topography of the ribbon.

SUPPLEMENTAL VIDEOS

Both videos have been captured during the same run, with $N = 167$ and $v = 0.1$ mm/s.

CompleteTightening.avi: example of a tightening of a Super 8 roll.

SlipEvent.avi: fast camera video of the slip event studied in Fig 5 in the main text.